Oxidative dehydrogenation of glycol to glyoxal on a P-modified electrolytic silver catalyst

Jingfa Deng, Jinhai Wang, Xinhua Xu
Department of Chemistry, Fudan University, Shanghai 200433, PR China

Hsing-Hua Huang and Guo-Qin Xu
Department of Chemistry, National University of Singapore, Singapore 0511

Received 10 July 1995; accepted 11 October 1995

A phosphorus-modified electrolytic silver catalyst was prepared and used as catalyst in the oxidative dehydrogenation of glycol to glyoxal. The yield of glyoxal was observed as high as 82% at 98% conversion for the Ag–P catalyst, while 62% at 89% conversion for the pure electrolytic silver. The formation of the surface compounds between the phosphorus additives and the silver surface was demonstrated by means of XPS and SEM. It caused the decrease of the surface concentration of atomic oxygen species, and restrained the decomposition and total oxidation of adsorbed glycol to C_1 products.

Keywords: glycol; oxidative dehydrogenation; silver–phosphorus catalyst

1. Introduction

Glyoxal is an important chemical product. Its aqueous solutions are manufactured either by nitric acid oxidation of acetaldehyde or by oxidative dehydrogenation of ethylene glycol. The latter reaction is more attractive because glycol can be obtained easily by hydrolysis of ethylene epoxide and the process is less polluting. The oxidative dehydrogenation of glycol is catalyzed by copper or silver catalysts, with high productivity. Both unsupported catalysts [1–6] and supported catalysts [7–10] are used. Most of the works mentioned above reported the use of promoters, especially phosphorous compounds, which were added into the reactant flow to increase the selectivity to glyoxal. A SiC supported silver catalyst was reported in the patents from Mitsui Toatsu where a 83% glyoxal yield at 99.9% conversion was claimed [7–10], and trace amounts of alkylphosphite compounds were used as promoters. Recently, Gallezot et al. [11] reported an intensive investigation for the effect of diethylphosphite (DEP) over SiC supported silver catalyst. They suggested that the addition of DEP decreased the probability of the reaction pathway leading to C_1 oxidized products by depleting the concentration of adsorbed oxygen. However, they revealed by various analyses that phosphorus, continuously injected in the form of DEP, did not remain on the catalyst. Therefore, the interaction between the phosphorus and the silver surface, and its effect on the oxygen adsorption and glycol oxidation is not unambiguous.

Electrolytic silver is a commercial catalyst for the manufacture of formaldehyde from methanol oxidation [12,13]. Our previous work [14] showed that a higher yield of formaldehyde was obtained on a phosphorus-modified electrolytic silver catalyst. A similar result was also reported by Aicher et al. [15]. Thus, the oxidation of glycol on the P-modified electrolytic silver catalyst is worth testing. On the other hand, the clean surface of electrolytic silver can be easily obtained and directly used to study the surface properties. By using an unsupported electrolytic silver catalyst, interaction between the silver and the support is avoided. Therefore, the investigation can focus on the interaction between the promoter P and the silver surface. In the present paper, we undertake a study combining physical characterizations of the Ag–P catalyst and the reaction data, which gives us a better understanding of the effect of the phosphorus additives on the selectivity to glyoxal.

2. Experimental

2.1. Sample preparation and materials

The electrolytic silver catalyst (purity 99.999%) was prepared by means of triple electrolytic refining. The preparation method as well as the surface structure of the electrolytic silver has been described in detail elsewhere [13]. As that for the industrial catalysts, the grain size of the silver is about 100 μm in diameter, with a specific surface area of 0.1 m^2/g, which does not change after catalytic reaction. The phosphorus was introduced into the silver by a conventional impregnation method in which phosphorus was chemically deposited from an aqueous solution of H_3PO_4 at room temperature. Then the catalyst was dried at 120°C and activated at 600°C for more than 3 h in air. The quantity of phosphorus in the catalyst, which was determined by ICP-AES, was controlled by changing the concentration of the H_3PO_4 solution.

2.2. Apparatus and procedures

Catalytic measurements were performed in a fixed-bed reactor. The reactor, a quartz tube with an i.d. of 18 mm, was loaded with 2–3 g catalyst. An aqueous solution of glycol was injected into a glass evaporator (250°C) by a micropump to be mixed with nitrogen and oxygen before entering the reactor. At 500°C, the space velocity was as high as 1.90×10^5 h^{-1} and the residence time in the catalyst bed was shorter than 0.02 s. The liquid products (e.g. glyoxal, glycol, formaldehyde, etc.) were quenched to room temperature and analyzed by chemical methods. The quantities of by-products, i.e. CO and CO_2 in the tail gas, were determined by a gas analyzer. The concentration of the glycol solution was determined by titration with HIO_4.

Surface analysis was carried out with a VG ESCALAB 5 electron energy spectrometer. The X-ray source used was Mg K_α. The energy analyzer was a double-pass, cylindrical mirror type analyzer (CMA). The pressure in the testing chamber was maintained at about 10^{-8} Pa during the experiments [16]. The spectra were obtained with a pass energy of 20 eV, providing an instrumental resolution of 0.2 eV. Binding energy measurements were calibrated by using $E_b(\text{Ag } 3d_{5/2}) = 368.0$ eV.

The SEM micrographs of the catalysts were obtained on a TSM-1 type scanning electron microscope. The pressure of the chamber was about 10^{-3} Pa.

3. Results and discussion

3.1. Catalytic measurements for the electrolytic silver catalyst with or without phosphorus additives

The experimental conditions chosen for the catalytic measurement were: reaction temperature: 500°C; concentration of inlet aqueous glycol: 50 wt%; space velocity (Vs): ~ 1.9×10^5 h^{-1}. The Vs was controlled by regulating the mole ratio of nitrogen to glycol and the amount of catalyst loaded.

The data of the changes in yield and conversion with the variation of mole ratio of oxygen to glycol on the pure electrolytic silver and on the electrolytic silver deposited with phosphorus content of 80 ppm are listed in tables 1 and 2, respectively. Different catalytic behaviors for these two kinds of catalysts are observed. In comparison with the pure silver catalyst, higher yield and selectivity to glyoxal are obtained on the silver–phosphorus (Ag–P) catalyst at mole ratios of oxygen to glycol above 1.30. But the conversion of glycol on the Ag catalyst is higher than that on the Ag–P catalyst at a given mole ratio of oxygen to glycol. This means that the addition of phosphorus onto the electrolytic silver causes the catalyst to become more selective and less active.

Fig. 1 shows the variation of the yield of glyoxal vs. the reaction temperature at various mole ratios of oxygen to glycol on the Ag–P catalyst. The best result is obtained at oxygen/glycol = 1.50 at 823 K, which is 83.4% selectivity to glyoxal at 97.9% conversion of glycol. This is consistent with the works by Mitsui Toatsu [7–10] and Gallezot et al. [11]. These results indicate that the phosphorus deposited onto a silver catalyst has the same promoting effect as the phosphorous compounds added into the reactant flow as promoters. Furthermore, the ICP-AES analysis of the P content of the Ag–P catalyst revealed that no detectable loss of phosphorus was observed after the catalytic reaction was conducted for more than 700 h, and the activity and selectivity were maintained. Therefore, the Ag–P catalyst prepared in the present investigation is stable, and the continuous addition of phosphorous promoters can be omitted. Thus, the phosphorus-modified electrolytic silver has potential as an industrial catalyst in the oxidative dehydrogenation of glycol to glyoxal.

The data in tables 1 and 2 show that the main by-products are HCHO and CO_2. In order to detect the origin of these C_1 products, blank experiments without catalysts were conducted with a 70 wt% glycol solution in the quartz reactor (mole ratio of oxygen/glycol of 1.20). Traces of glyoxal were detected and the main products were formaldehyde and CO_2. The yields of HCHO and CO_2 at 500°C were 15.5 and 6.0%, respectively, and

Table 1
The effect of mole ratio of oxygen to glycol on activity of Ag catalyst [a]

Run	Mole ratio of oxygen to glycol	Conversion of glycol (mol%)	Yield of products (mol%)			Selectivity of glyoxal (mol%)
			$(CHO)_2$	HCHO	CO_2	
1	0.97	79.3	50.6	13.4	15.1	63.8
2	1.07	85.1	56.1	8.7	20.1	65.9
3	1.23	88.9	62.1	4.1	22.5	69.9
4	1.35	94.2	60.5	9.4	24.1	64.2
5	1.45	95.8	56.7	11.5	27.3	59.2
6	1.56	99.4	50.8	14.5	34.0	51.1

[a] Reaction conditions: concentration of aqueous glycol: 50 wt%; reaction temperature: 500°C; mole ratio of nitrogen to glycol: 64.1; space time: 52.3 s^{-1}.

Table 2
The effect of mole ratio of oxygen to glycol on activity of Ag–P catalyst [a]

Run	Mole ratio of oxygen to glycol	Conversion of glycol (mol%)	Yield of products (mol%)			Selectivity of glyoxal (mol%)
			$(CHO)_2$	HCHO	CO_2	
1	1.02	59.8	37.6	19.7	2.1	62.8
2	1.15	74.0	52.4	17.4	3.7	70.8
3	1.36	89.5	70.8	13.4	5.6	76.2
4	1.50	95.9	78.2	10.4	7.0	81.3
5	1.73	97.9	76.2	7.6	13.9	77.8
6	1.91	99.9	70.0	6.8	22.8	70.1

[a] Reaction conditions: concentration of aqueous glycol: 50 wt%; reaction temperature: 500°C; mole ratio of nitrogen to glycol: 86.0; space time: 54.1 s^{-1}.

those at 200°C were 8.0 and 0.0%. These data are approximately equal to those obtained on the Ag–P catalyst (table 2, runs 2 and 3). It seems that the C_1 products are formed via the homogeneous gaseous reaction between glycol and oxygen, rather than via the catalytic reaction on the surface of Ag–P. However, the presence of the Ag catalyst in the reactor caused a great increase of CO_2 yield and simultaneous decrease of HCHO yield (table 1, run 3). This result implies that the electrolytic silver catalyzes the total oxidation to CO_2, and it is consistent with the work by Gallezot et al. [11], in which they revealed that metals, even the wall of the stainless steel reactor, would catalyze the decomposition and oxidation of glycol. Therefore, we can conclude that the addition of phosphorus onto the electrolytic silver restrains the total oxidation reaction pathway, which is catalyzed by a pure Ag surface, and this improves the selectivity to glyoxal.

3.2. XPS and SEM results

XPS was used to investigate the interaction between the phosphorus additives and the silver surface. In the process of preparing the Ag–P catalyst, H_3PO_4 was deposited onto the electrolytic silver and the Ag–P catalyst thus prepared was dried and activated at up to 600°C. Fig. 2 shows the P_{2p} core spectra of the Ag–P catalyst at various activation temperatures. After drying at 120°C, the P_{2p} spectrum shows a single peak centered at the binding energy of 134.5 eV. Two peaks can be observed when the Ag–P catalyst is heated up to a temperature of 250°C, centered at 134.0 and 132.6 eV, respectively. The intensity of the peak at 132.6 eV increases with increasing activation temperature, while the peak at 134.0 eV decreases and almost disappears

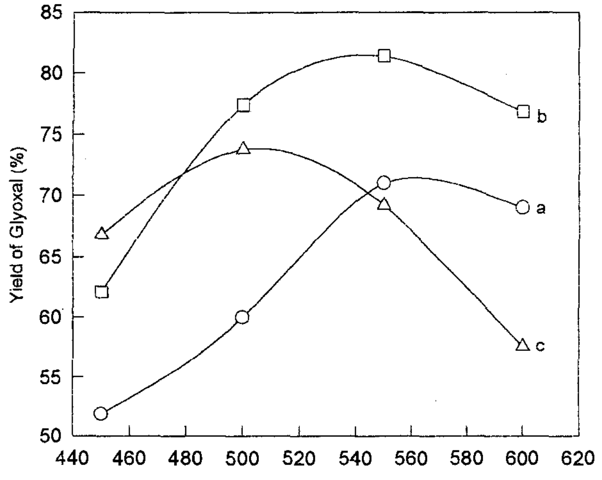

Fig. 1. The effect of reaction temperatures on yield of glyoxal mole ratio of oxygen to glycol: (a) 1.1, (b) 1.5, (c) 1.9.

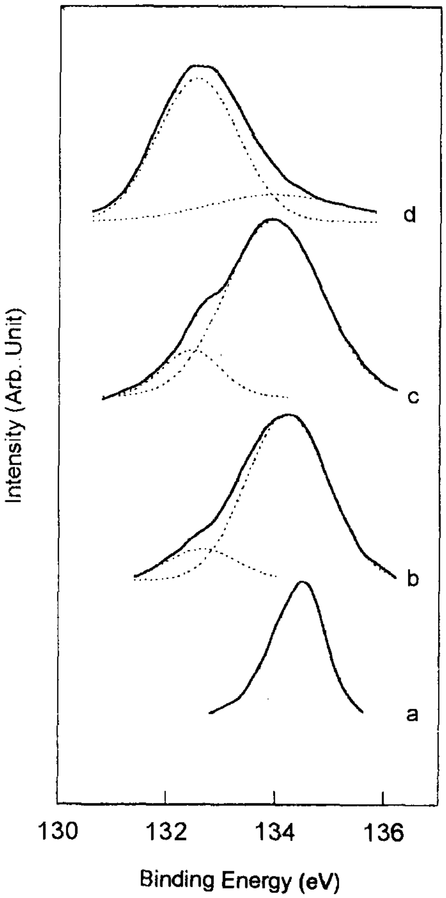

Fig. 2. P_{2p} XPS spectra of Ag–P catalyst after activiation at various temperatures. Activiation temperature: (a) 120°C, (b) 250°C, (c) 400°C, (d) 550°C.

after activating at 550°C. In order to identify the state of phosphorus additives, a variety of phosphoric compounds were chemically deposited on the electrolytic silver and the P_{2p} spectra of these compounds were obtained under the same conditions. The results are listed in table 3, as well as the data reported in ref. [17]. Thus, we can see that phosphorus is deposited in the form of phosphoric acid (H_3PO_4) on an unactivated silver catalyst (dried at 120°C). By raising the activation temperature, H_3PO_4 dehydrates and interacts with the silver surface to produce a series of phosphorate salts. At 550°C, E_b of P_{2p} becomes 132.6 eV which means that phosphorus exists predominantly in the form of phosphate salts. In order to investigate the changes of these surface compounds during the reaction, we also measured the Ag $3d_{5/2}$ XPS spectra. The binding energy of Ag $3d_{5/2}$ for the electrolytic silver and Ag_3PO_4 powders was obtained at 367.9 and 368.2 eV, respectively. Since it was difficult to distinguish these two species from each other, the difference spectra of Ag $3d_{5/2}$ between the Ag–P and Ag catalyst are presented in fig. 3. It can be seen that after activation at 550°C, there are two states of Ag, with binding energies of 367.4 and 368.2 eV, respectively. The peak at 367.4 eV is assigned to Ag_2O on the surface. After the catalyst was used in the catalytic process, the Ag_2O decomposed and the peak at 368.2 eV became obvious. This result also implies that there is a strong interaction between the phosphorus and the silver surface and that some kind of phosphorate salt, such as Ag_3PO_4, is formed on the electrolytic surface.

The XPS measurement shows that the surface phosphorus content of the Ag–P catalyst decreased in the initial stage of catalytic reaction. However, the ICP-atomic emission spectra results show that the total amount of P in the Ag–P catalyst does not change during the reaction. Therefore, we suggest that P dissolves into the bulk of the electrolytic silver. Then surface content and the binding energy of the phosphoric species is constant during the reaction for more than 700 h, and the activity of the catalyst shows no obvious change. This result supports the above conclusion that a stable surface compound has been formed between the phosphorus additives and the silver surface.

The interaction between the added phosphorus and the silver surface can also be observed by scanning electron microscope measurements. Fig. 4a is the SEM micrograph of the electrolytic silver, which shows a pile of silver branches with smooth surfaces. The SEM micrograph for Ag–P dried at 120°C is shown in fig. 4b. The morphological configuration of the unactivated Ag–P catalyst shows the broken pieces of silver plate deposited with small particles, which are suggested to be H_3PO_4 microcrystals. The SEM micrographs for Ag and Ag–P catalysts after activating at 550°C are shown in figs. 5a and 5b. The electrolytic silver surface is smooth and melted, while the surface of Ag–P consists of holes and terraces, which are suggested to be caused by corrosion of the silver surface by H_3PO_4. These results confirm directly that the deposited H_3PO_4 dehydrates and reacts with the silver surface intensively as the activation temperature increased.

Table 3
Binding energies of P_{2p} (eV) for a variety of phosphoric compounds

Compound	E_b [a] (eV)	E_b [b] (eV) in ref. [17]
H_3PO_4	134.4	–
$H_4P_2O_7$	135.0	–
HPO_3	135.3	–
Na_3PO_4	132.6	132.3
Na_2HPO_4	133.6	132.9
NaH_2PO_4	133.7	133.4(KH_2PO_4)
$Na_4P_2O_7$	133.0	132.9
$NaPO_3$	134.1	134.1

[a] Calibrated by Ag $3d_{5/2}$ = 368.0 eV.
[b] Ag $3d_{5/2}$ = 367.9 eV.

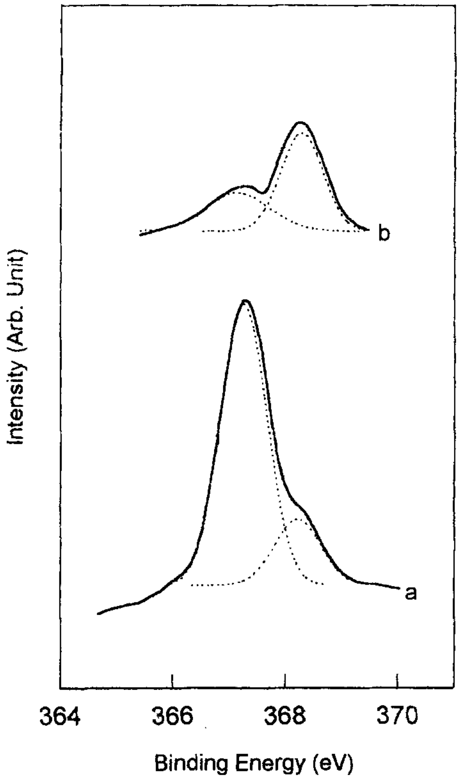

Fig. 3. The difference spectra of Ag $3d_{5/2}$ between Ag–P catalyst and electrolytic silver catalyst. (a) Ag–P as-prepared, (b) Ag–P after treatment under the reaction conditions.

According to the molecular mechanism of glycol adsorption and conversion on Ag(110) single crystalline surface by Capote and Madix [18,19], the first step is that glycol reacts with surface oxygen to form water and adsorbed 1,2-diethanedioxy species ($OCH_2CH_2O(a)$):

$$HOCH_2CH_2OH(g) \rightarrow HOCH_2CH_2OH(a) \tag{1}$$

$$HOCH_2CH_2OH(a) + O(a) \rightarrow HOCH_2CH_2O(a) + OH(a) \tag{2}$$

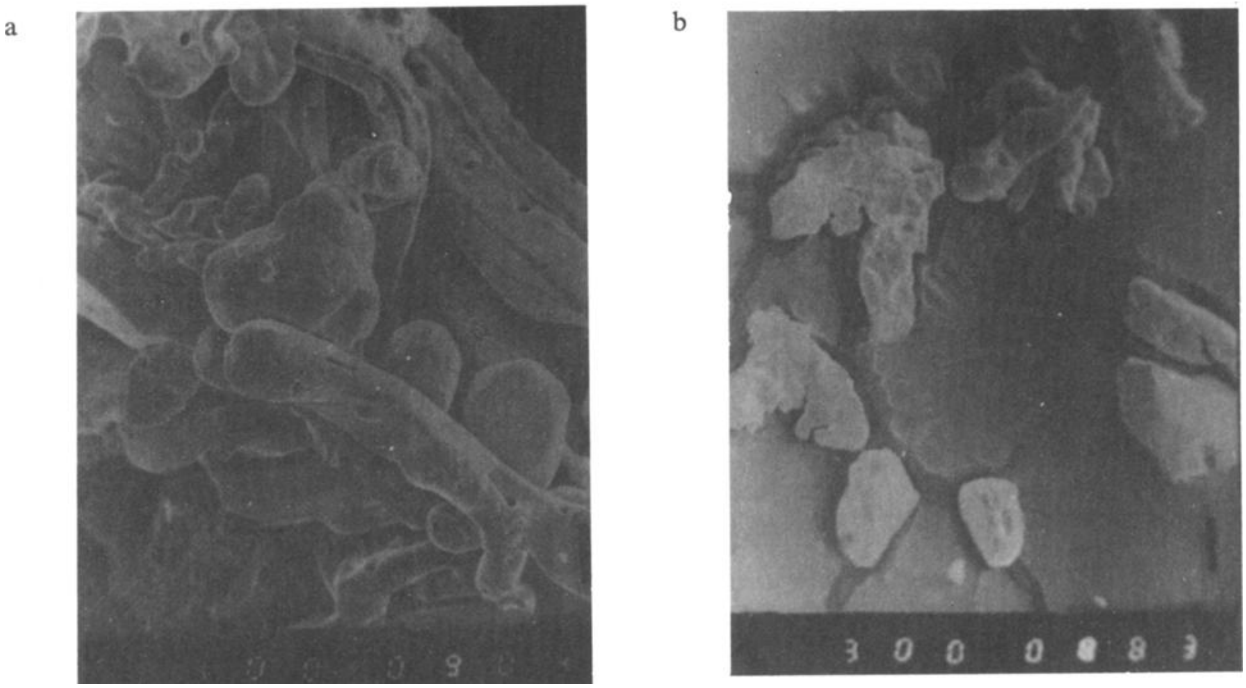

Fig. 4. The SEM micrograph of electrolytic silver and unactivated Ag–P catalyst (×300). (a) Electrolytic silver, (b) unactivated Ag–P catalyst.

$$HOCH_2CH_2O(a) + OH(a) \rightarrow OCH_2CH_2O(a) + H_2O(a) \quad (3)$$

The diethanedioxy species can dehydrogenate into glyoxal by breaking the C–H bond:

$$OCH_2CH_2O(a) \rightarrow OCH_2CH{=}O(a) + H(a) \quad (4)$$

$$OCH_2CH{=}O(a) \rightarrow O{=}CHCH{=}O(g) + H(a) \quad (5)$$

Further reaction of $OCH_2CH_2O(a)$ with surface oxygen via rate-limiting C–C bond breaking yields water, formaldehyde and adsorbed formate species:

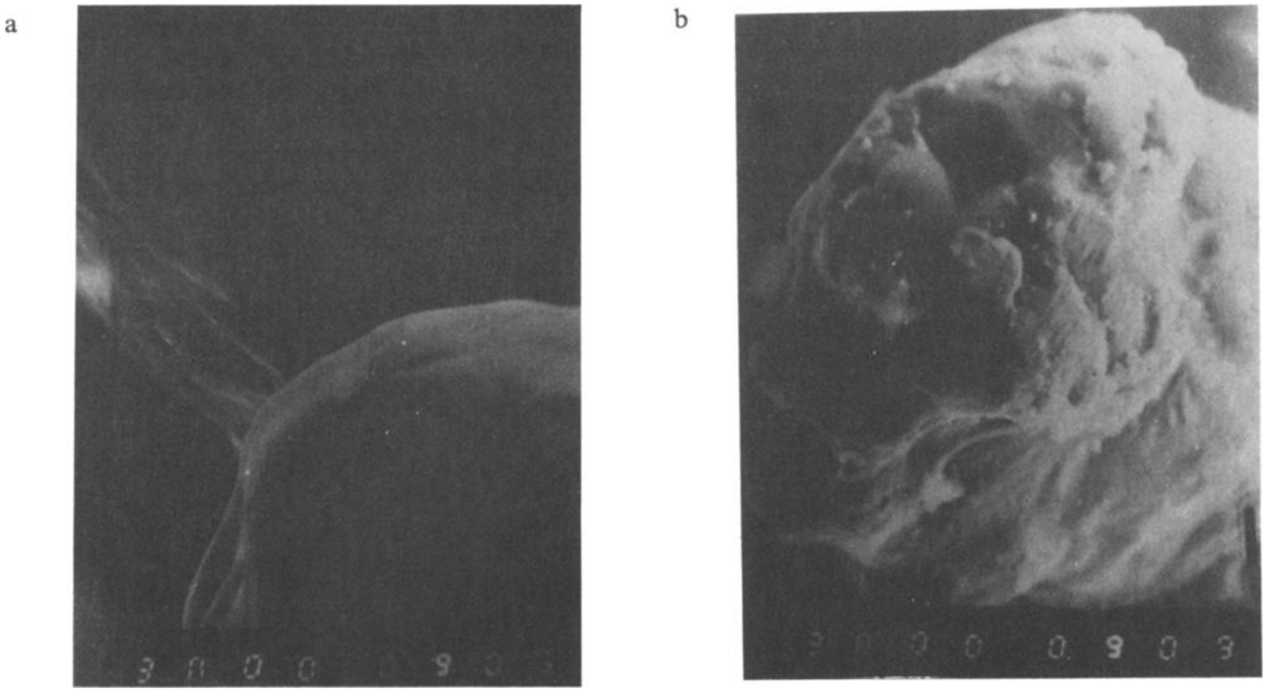

Fig. 5. The SEM micrograph of electrolytic silver and Ag–P catalyst after activating at 550°C (×3000). (a) Electrolytic silver, (b) Ag–P catalyst.

$$\mathrm{OCH_2CH_2O(a) + O(a)} \rightarrow \mathrm{O{=}CHCH_2O(a) + OH(a)} \qquad (6)$$

$$\mathrm{OCH_2CH_2O(a) + OH(a)} \rightarrow \mathrm{O{=}CHCH_2O(a) + H_2O(g)} \qquad (7)$$

$$\mathrm{O{=}CHCH_2O(a) + O(a)} \rightarrow \mathrm{HCOO(a) + H_2C{=}O(g)} \qquad (8)$$

and subsequently CO or CO_2 are formed:

$$\mathrm{HCOO(a) \rightarrow CO_2(g) + H(a)} \qquad (9)$$

$$\mathrm{H_2CO(g) \rightarrow CO(g) + H_2(g)} \qquad (10)$$

This mechanism has also been investigated and confirmed in our laboratory on the electrolytic silver surface [20]. Thus, the concentration of the surface oxygen plays an important role in controlling the reaction extent of dehydrogenation or oxidation of the $OCH_2CH_2O(a)$ species, which determines the selectivity of the reaction. Gallezot et al. [11] suggested that the addition of DEP decreased the amount of adsorbed atomic oxygen to a level where reactions (6)–(8) leading to C_1 products became less probable, thus increasing the amount of glyoxal production via reactions (4) and (5). However, the details of this kind of effect were not clear since they found that DEP could not remain on the Ag/SiC catalyst.

In the present work, we have shown the P-modified electrolytic silver is an effective catalyst for the oxidative dehydrogenation of glycol to glyoxal. An interaction between the phosphorus additives and the silver surface has also been observed by XPS and SEM. This interaction affects the characteristics of the adsorbed oxygen. The XPS spectra of oxygen on electrolytic silver (fig. 6) showed that at room temperature at least three different oxygen states existed on the sample with an exposure of 2×10^2 L ($P_{O_2} = 1.2 \times 10^{-7}$ Torr). The binding energies of the O_{1s} core level were about 528.5, 530.2 and 532.0 eV, respectively. The XPS subtraction spectra between the two different exposures are given in fig. 7. It is seen that the peak at $E_b = 528.3$ eV grew as the oxygen exposure increased from 10^2 to 10^3 L, but it decreased and a new peak at 529.7 eV appeared simultaneously when the exposure increased further to 10^5 L ($P_{O_2} = 6 \times 10^{-5}$ Torr). Then, at an exposure of 10^6 L ($P_{O_2} = 7.5 \times 10^{-4}$ Torr), the 530.2 eV peak with a shoulder peak at 532.2 eV appeared. Finally, for even higher exposure, the peak at 530.2 eV increased in intensity. The peak at 532.2 eV is assigned to molecular oxygen on the silver surface [21,22]. The peaks at 528.3 and 529.7 eV are due to adsorbed atomic oxygen. The fact that the peak at 532.2 eV remained unchanged when the peak at 528.3 eV diminished and the peak at 529.7 eV appeared indicates that the adsorbed atomic oxygen

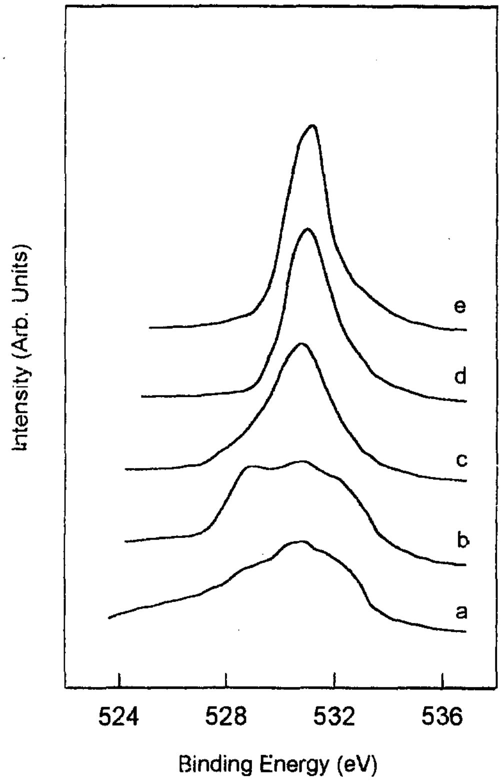

Fig. 6. The O_{1s} XPS spectra of oxygen on electrolytic silver catalyst at various exposures of oxygen: (a) 2.1×10^2 L, (b) 4.0×10^3 L, (c) 1.1×10^5 L, (d) 1.4×10^6 L, (e) 1.7×10^9 L.

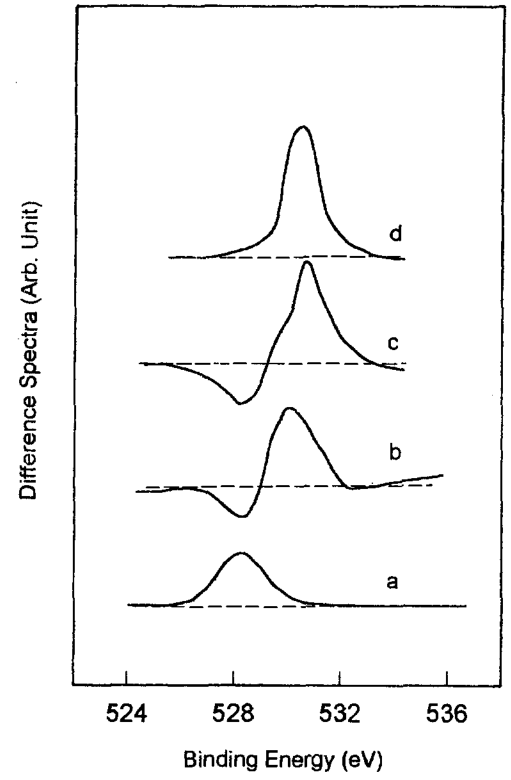

Fig. 7. Difference spectra of O_{1s} for various exposures of oxygen. (a) 4.0×10^3 to 2×10^2 L, (b) 1.1×10^5 to 4.0×10^3 L, (c) 1.4×10^6 to 1.1×10^5 L, (d) 1.7×10^9 to 1.4×10^6 L.

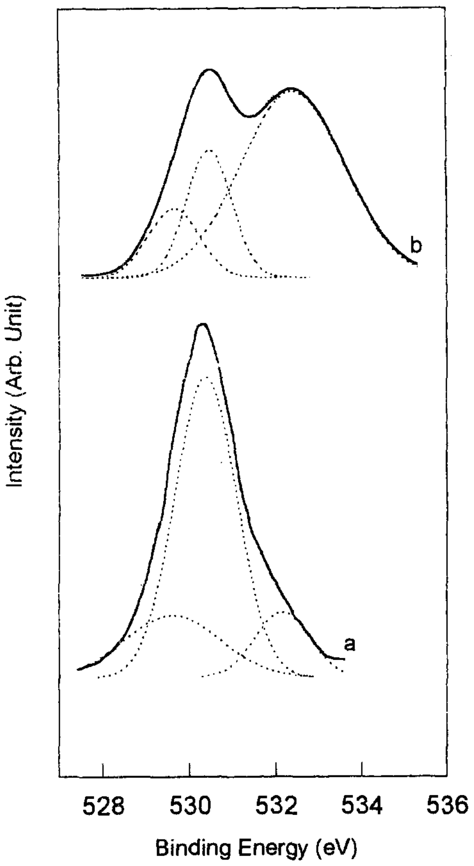

Fig. 8. The O_{1s} XPS spectra of oxygen adsorbed on electrolytic silver and Ag–P catalyst. (a) After exposure of 1.4 × 10^6 L oxygen onto electrolytic silver, (b) the difference spectra of the Ag–P surface after exposing 1.6 × 10^7 L oxygen to that of the Ag–P surface without exposing oxygen.

Table 4
The O_{1s} XPS peak parameters of oxygen adsorbed on the Ag and Ag–P catalyst surfaces

Catalyst	Binding energy (eV)	FWHM (eV)	Area (arb. unit)	s (%)
electrolytic silver	529.7	2.03	2850	19.8
	530.4	1.43	9650	67.0
	532.1	1.28	1900	13.2
Ag–P catalyst	529.6	1.18	1820	11.6
	530.5	1.35	3850	24.5
	532.3	2.42	10050	63.9

does not tend to recombine to form molecular oxygen but rather forms another phase of atomic oxygen as the coverage increases. This is consistent with the results of Cyanderna [23]. Continuous increase of the oxygen exposure enhanced the peak at 530.2 eV. This implies that the oxygen species corresponding to 530.2 eV pertains to sub-surface atomic oxygen [21]. These characteristics of the adsorbed oxygen on electrolytic silver have also been investigated intensively by TDS, UPS, HREELS and work function measurements in our laboratory [24,25].

Therefore, the dominant trend of oxygen adsorption on electrolytic silver is to form surface and sub-surface atomic oxygen, the high surface concentration of which causes the decomposition and total oxidation of glycol to C_1 products. By adding H_3PO_4 onto the electrolytic silver, a strong interaction between P and Ag is observed and the characteristics of adsorbed oxygen are changed. The XPS spectra of the O_{1s} core level for adsorbed oxygen on the Ag–P catalyst is presented in fig. 8 as well as that on the pure Ag catalyst. Table 4 lists the parameters of the XPS peaks shown in fig. 8. It is seen that the states of the adsorbed oxygen on Ag–P are the same as those on pure Ag catalyst, e.g. molecular oxygen (whose XPS peaks are at 532.3 eV), surface and sub-surface atomic oxygen (whose XPS peaks are at 529.6 and 530.5 eV, respectively). Excluding from consideration the sub-surface atomic oxygen species, it can be estimated from the data in table 4 that the ratio of surface molecular oxygen to atomic oxygen on Ag and Ag–P is 0.67 and 5.52, respectively. This means that the molecular oxygen adsorbed on Ag–P catalyst is difficult to dissociate into atomic oxygen species. It can also be seen that in order to reach an O_{1s} peak of approximately equal intensity, the oxygen exposure onto Ag–P should be 10 times higher than that onto pure Ag catalyst. Furthermore, we can estimate that the total amount of adsorbed oxygen on Ag–P is only 1/10–1/2 of that on electrolytic silver catalyst at the same oxygen exposure. Thus, it can be suggested that the surface concentration of atomic oxygen is reduced by addition of P onto the electrolytic silver, and that this restrains the reaction pathways towards C_1 products and increases the selectivity to glyoxal.

4. Conclusion

In the present work, we develop a P-modified silver catalyst which shows high activity and selectivity for the oxidative dehydrogenation of glycol to glyoxal. A stable surface compound was formed by strong interaction between the phosphorus and the silver surface. This decreases the surface concentration of atomic oxygen and restrains the reaction pathway towards C_1 products. The Ag–P catalyst has been operated for more than 700 h and its activity and selectivity are constant.

Acknowledgement

This work was supported by grants of the National Natural Science Foundation of China.

References

[1] Carbide and Carbon, US 2,339,282 (1940).
[2] Laporte, DE 1,923,048 (1968); DE 1,967,147 (1968).

[3] American Cyanamid, DE 2,634,439 (1975).
[4] BASF, EP 3,443 (1978); EP 19,772 (1979); EP 72,912 (1981); EP 287,884 (1987).
[5] Nippon Goshei, DE 3,904,829 (1989).
[6] Mitsubishi, JP 59-203928 (1982).
[7] Mitsui Toatsu, JP 58-38277 (1981); JP 58-59933 (1981).
[8] Mitsui Toatsu, US 4,555,583 (1985).
[9] Mitsui Toatsu, JP 60-100533 (1983).
[10] Mitsui Toatsu, JP 91-232835 (1991).
[11] P. Gallezot, S. Tretjak, Y. Christidis, G. Mattioda and A. Schouteeten, J. Catal. 142 (1993) 729.
[12] M.A. Barteau and R. J. Madix, in: *Chemical Physics of Solid Surface and Heterogeneous Catalysis*, Vol. 4, eds. D.A. King and D.P. Woodruff (Elsevier, Amsterdam, 1982) p. 100.
[13] X. Bao and J.F. Deng, J. Catal. 99 (1986) 391.
[14] X. Bao, J.F. Deng and X. Dong, Acta Chim. Sinica 44 (1986) 619.
[15] A. Aicher, W. Disteldort, N. Petri and G. Reuss, Eur. Pat. Appl. EP 467,169 (1992).
[16] X. Bao, J.F. Deng and S. Dong, Surf. Sci. 163 (1985) 444.
[17] C.D. Wagner, W.M. Riggs, L.E. Davis, J.F. Moulder and G.E. Muilenberg, in: *Handbook of X-ray Photoelectron Spectroscopy* (Perkin-Elmer Corp., Phys. Electr. Div., 1978).
[18] A.J. Capote and R.J. Madix, J. Am. Chem. Soc. 111 (1989) 3570.
[19] A.J. Capote and R.J. Madix, Surf. Sci. 214 (1989) 276.
[20] J. Wang and J.F. Deng, J. Catal. (Chinese, Cuihua Xuebao) 15 (1994) 250.
[21] R.W. Joyner and M.W. Roberts, Chem. Phys. Lett. 60 (1979) 459.
[22] C.N.R. Rao, P.V. Kamath and S. Yashonath, Chem. Phys. Lett. 88 (1982) 13.
[23] A.W. Cyanderna, J. Vac. Sci. Technol. 14 (1977) 408.
[24] X. Bao, S. Dong and J.F. Deng, Surf. Sci. 199 (1988) 493.
[25] X. Bao, J.F. Deng, R. Zhai, D. Wang and X. Guo, Catal. Lett. 4 (1990) 25.